Supplement of Atmos. Meas. Tech., 13, 6193–6213, 2020
https://doi.org/10.5194/amt-13-6193-2020-supplement

Atmospheric Measurement Techniques
Open Access

Supplement of

Interferences with aerosol acidity quantification due to gas-phase ammonia uptake onto acidic sulfate filter samples

Benjamin A. Nault et al.

Correspondence to: Jose L. Jimenez (jose.jimenez@colorado.edu)

S1. GEOS-Chem Model

We used a global chemical transport model (GEOS-Chem 11-02-rc, (Bey et al., 2001)) to estimate sulfate mass concentration distributions in the troposphere. The GEOS-Chem model was driven by assimilated meteorological fields from the Goddard Earth Observing System Forward Processing (GEOS-FP) for a year (May 2013 to June 2014, with the first two months discarded for spin-up). The simulation was conducted at 2° (latitude)×2.5° (longitude) with 47 vertical layers up to 0.01 hPa and ~30 layers under 250 hPa. We used the EDGAR v4.3 global anthropogenic emissions (Crippa et al., 2018). The global fire emissions database version 4 (GFED4) was used for biomass burning emissions (Giglio et al., 2013). Gas-particle partitioning of inorganic aerosols was calculated with the ISORROPIA II thermodynamic model (Fountoukis and Nenes, 2007; Pye et al., 2009), but we excluded sea salt in the ISORROPIA calculation based on Nault et al. (2020).

S2. SAGA Filter Extraction

The 20 mL is thought to be a balance between a couple of competing factors. (1) The SAGA team wants to be confident that they are completely extracting the soluble material from the filters (recall, the filters are 90 mm in diameter). They had conducted testing when they first started operating on the NASA DC-8 (late 1980's-early 1990's) and established that this amount of water was necessary to fully extract the material. (2) To counter the dilution, the SAGA team uses a pre-concentrator column and large volume injections into the IC (~5 mL). These two aspects compensate for the greater dilution. (3) Finally, 5 mL is injected for both anions and cations (total 10 mL), and enough sample is left to conduct a follow-up injection if there was any concern about the data.

S3. Equations for the Ammonia Flux Model

$$v_{NH_3} = \sqrt{\frac{8 \times k_B \times T_{cabin} \times 1000 \times Av}{\pi \times MW_{NH_3}}} \quad \text{Eq. S1}$$

$$AeroConc = \frac{\frac{4}{3} \times \pi \times (0.5 \times D_{particle} \times 10^{-7})^3 \times \rho_{particle} \times Av}{MW_{particle}} \quad \text{Eq. S2}$$

$$NH_{3,Flux} = \pi \times (0.5 \times D_{particle} \times 10^{-9})^2 \times v_{NH_3} \times \alpha \times [NH_3] \times (J/J_c) \quad \text{Eq. S3}$$

$$Time = \frac{AeroConc}{NH_{3,Flux}} \quad \text{Eq. S4}$$

Above, are the equations used in the theoretical ammonia uptake model (Sect. 2.4) (Seinfeld. and Pandis, 2006). v_{NH_3} (Eq. S1) is the velocity of ammonia gas (m/s). AeroConc (Eq. S2) is the aerosol concentration, in molecules, for a given aerosol diameter. $NH_{3,Flux}$ (Eq. S3) is the flux of ammonia (molecule s^{-1}). Finally, *Time* is the time needed for one ammonia molecule to interact with one sulfuric acid (s).

The remaining variables are defined here. In Eq. S1, k_B is the Boltzmann constant (1.38×10^{-23} J K^{-1}), T_{cabin} is the temperature in the cabin of the DC-8 (298 K), *Av* is Avogrado's number (6.02×10^{23} molecules mol^{-1}), MW_{NH3} is the molecular weight of gas-phase ammonia (17 g mol^{-1}), and the 1000 is a conversion factor from g to kg. For Eq. S2, $D_{particle}$ is the diameter of the particle in nm (100 – 1000 nm), 10^{-7} is a conversion factor from nm to cm, $\rho_{particle}$ is the density of sulfuric acid (1.8 g cm^{-3}), and $MW_{particle}$ is the molecular weight of sulfuric acid (98 g mol^{-1}). In Eq. S3, $D_{particle}$ is the diameter of the particle (100 – 1000 nm), 10^{-9} is a conversion factor from nm to m, v_{NH_3} is from Eq. S1 (m/s), α is the accommodation coefficient for ammonia with sulfuric acid (1), $[NH_3]$ is the concentration of ammonia in ppbv, and J/J_c is the Fuchs-Sutugin correction for a transition regime.

The above equations assume a spherical aerosol on the filter. It is possible that the liquid particle adopts a more elongated shape upon contact with the filter fiber. To estimate the impact of change of liquid aerosol into more cylindrical shape, we use the following equations:

$$volume_{cylinder} = volume_{sphere} \quad \text{Eq. S5}$$

$$r_{cylinder} = \sqrt{volume_{sphere}/(\pi h_{cylinder})} \quad \text{Eq. S6}$$

where r is the radius of the sphere, $r_{cylinder}$ is the radius and $h_{cylinder}$ is the height for the cylinder. We assume volume of the sphere is conserved, and take a few values for $h_{cylinder}$: $h_{cylinder}$ is 1 nm, $h_{cylinder}$ is 25 nm, or $h_{cylinder}$ is radius of the sphere. $r_{cylinder}$ from Eq. S6 is then used in Eq. S3 to calculate flux.

S4. Estimated Influence of Ammonia Offgasing from Polyethylene Bags

Research from co-authors on a prior paper showed that films of water are the most likely reason for the retention and slow release of sticky volatile gases from surfaces coated by Teflon and other surfaces. An upper limit water thickness is ~10 µm (Liu et al., 2019). The Henry's Law Coefficient for ammonia is 62 M atm^{-1} (Seinfeld. and Pandis, 2006). With the bags being

~1.6×10^{4} mm^2 (~1.6×10^{-2} m^2), that would put an upper limit of water volume of ~1.6×10^{-7} m^3 (~1.6×10^{-4} L). The average ammonia in the cabin of the DC-8 was ~45 ppbv (~4.5×10^{-9} atm), leading to ~2.8×10^{-7} M ammonia partitioned to the water in the bag. Thus, that would lead to ~4.5×10^{-11} mol ammonia on the walls, or ~2.7×10^{13} molecules ammonia. The average number of sulfate molecules on the filters was ~3.8×10^{15}. Thus, at the upper limit for the water thickness of the bags, there is ~0.7% ammonia:sulfate molecules. As the bags are blown with dry air prior to placing the filters into the bags, the water thickness is expected to be lower (~0.1 µm), leading to a three order magnitude decrease for ammonia molecules in the bag. Thus, the bags are not expected to be a large source of ammonia contamination. However, this effect has not been directly investigated.

S5. DC-8 Cabin Air Exchange Rates

Air inside the cabin of the DC-8 is constantly being exchanged with ambient air to minimize build-up of carbon dioxide mixing ratios from human emissions, to increase comfort, and to improve human health (Hunt and Space, 1994; Hocking, 1998; Brundrett, 2001; National Research Council, 2002). This exchange rate is factors to an order of magnitude higher than the exchange rates in typical indoor environments (Hunt and Space, 1994). The exchange rate will impact the ammonia mixing ratio in the cabin, as ambient ammonia can be drawn into the airplane and the ventilation will generally reduce the ammonia mixing ratio due to human emissions, similar to carbon dioxide.

To calculate the exchange rate, a mass balance method . (Pagonis et al., 2019) was used where the cabin of the DC-8 is assumed to be well-mixed (Eq. S7 and Eq. S8 below). For this method, ambient carbon dioxide, measured by AVOCET (Vay et al., 2003, 2011), and cabin carbon dioxide, measured by the HOBO MX1102 Carbon Dioxide Data Logger, were used. The maximum number of passengers on the NASA DC-8 during FIREX-AQ was 40 people, which is used in this calculation. Finally, the volume of the portion of the DC-8 accessed by passengers is ~258 m^3 (Anon, 2011). These values are used in Eq. S7 and Eq. S8 to estimate the exchange rate. Here, we assumed that carbon dioxide was in steady-state to estimate the air exchange rate.

$$\frac{dCO_{2,DC-8}}{dt} = \frac{AER_{DC-8}([CO_{2,ambient}]-[CO_{2,DC-8}])+(E_{CO_2,Person}\times N)}{V_{DC-8}} \quad \text{Eq. S7}$$

$$AER_{DC-8} = \frac{(-(E_{CO_2,Person}\times N)/V_{DC-8})}{([CO_{2,ambient}]-[CO_{2,DC-8}])} \quad \text{Eq. S8}$$

Above, for Eq. S7 and Eq. S8, AER_{DC-8} is the air exchange rate, in hr^{-1}, $[CO_{2,ambient}]$ is the ambient mixing ratio of carbon dioxide, $[CO_{2,DC-8}]$ is the carbon dioxide mixing ratio in the cabin of the DC-8, $E_{CO2,Person}$ is the emission rate of carbon dioxide per person (21 g hr^{-1} $person^{-1}$ (Tang et al., 2016)), N is the number of people in the cabin (40), and V_{DC-8} is the volume of the cabin (258 m^3).

After solving for the exchange rate (AER_{DC-8}), Eq. S8 can be rearranged to estimate the mixing ratio of ammonia in the cabin of the DC-8. Using 1940 µg hr^{-1} $person^{-1}$ as the ammonia emission rate per person, the cabin ammonia mixing ratio is 43.4 ppbv. There have been minimal studies (two to the best of our knowledge) that have measured total ammonia emissions from human activity. For one study, which investigated the emissions from hard activity (workout), the value of 1940 µg hr^{-1} $person^{-1}$ is at the lower end (Finewax et al., 2020); however, the total human emissions during this study were potentially higher to higher sweating from exercise, which leads to the hydrolysis of urea to form gas-phase ammonia (Healy et al., 1970; Sutton et al., 2000). For the other study that measured total ammonia emission (Li et al., 2020), the value of 1940 μg hr^{-1} $person^{-1}$ is similar to the values observed for humans doing low to medium activity.

Figures

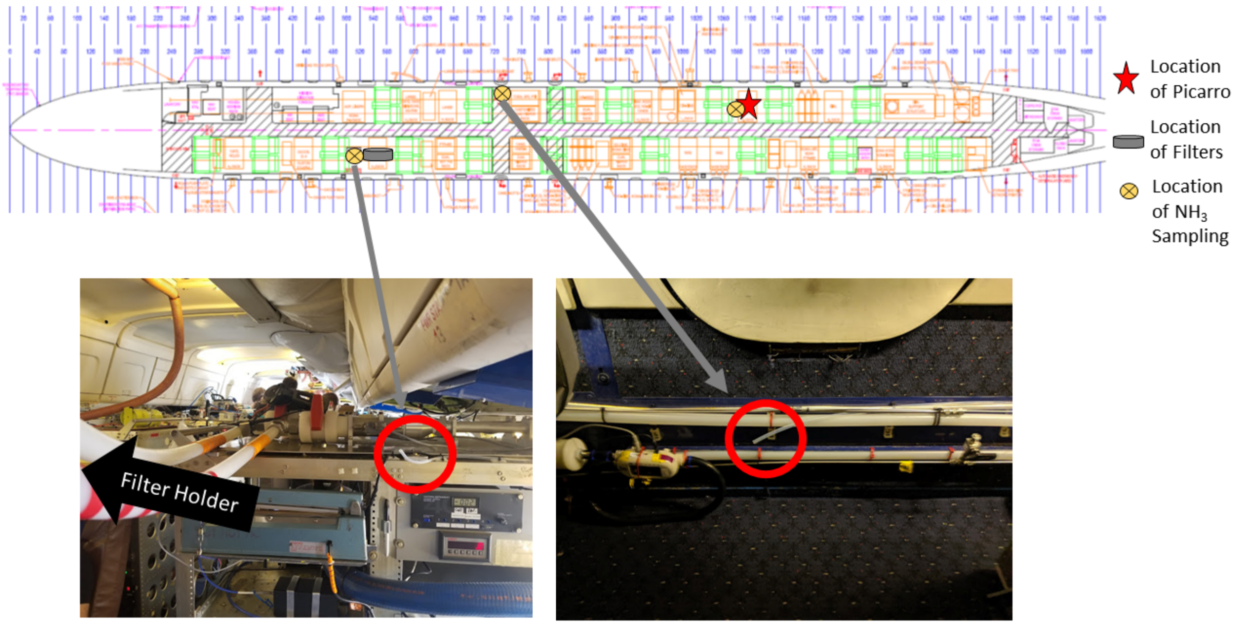

Figure S1. (Top) Floor plan of the DC-8 for the FIREX-AQ campaign (Webster, 2019). Location of where the Picarro instrument, aerosol filter sampling, and sampling of cabin ammonia locations (red circles) during the campaign are shown. Photos of the sampling by the filter collection (bottom left) and mid-cabin sampling (bottom right) are shown. The actual filter holder in the bottom left is in the direction of the arrow and not pictured.

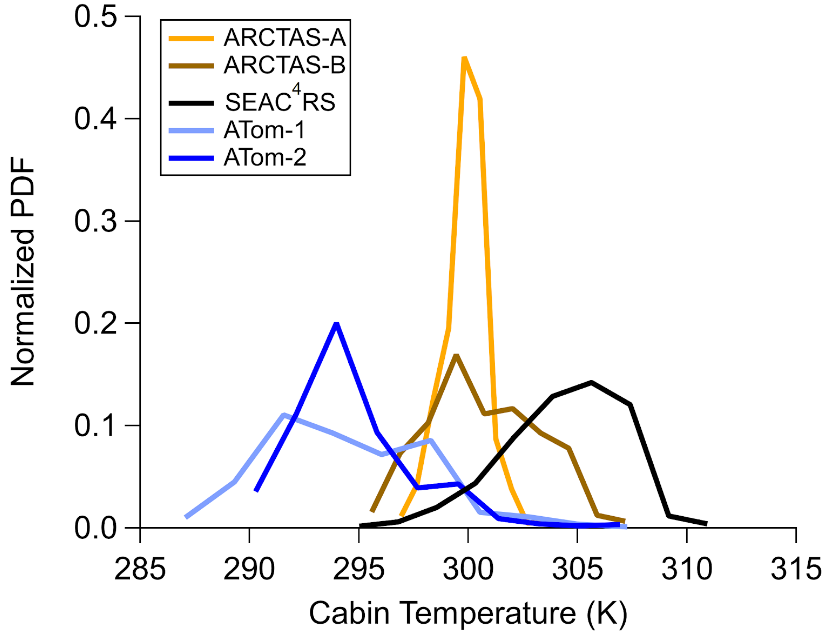

Figure S2. Normalized probability distribution function (PDF) of cabin temperature (K) during five aircraft campaigns.

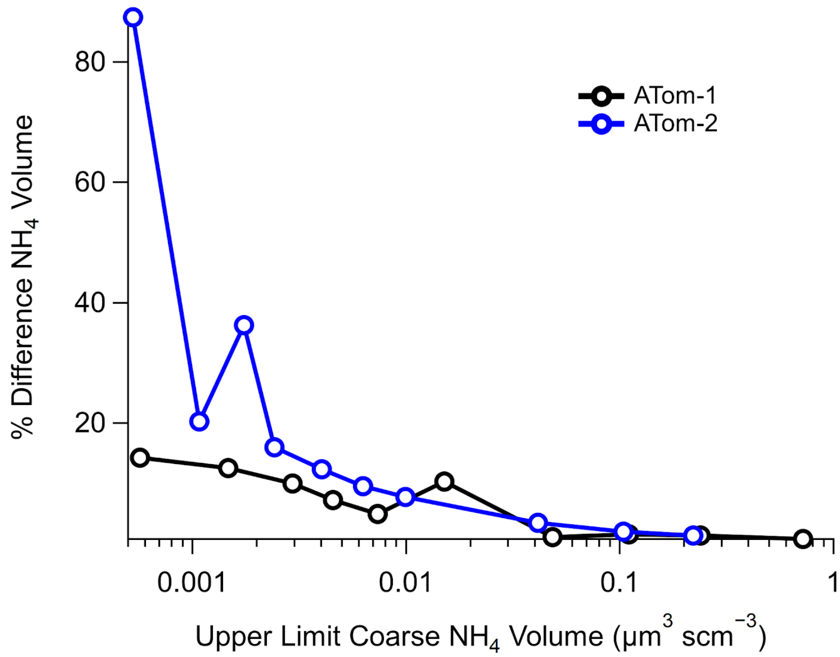

Figure S3. Percent difference in measured ammonium volume (((filter NH_4 - AMS NH_4)/1.78)/(AMS NH_4/1.78)×100) versus upper limit coarse NH_4 volume. The 1.78 is the density of ammonium in g cm^{-3} (Rumble, 2019), and the upper limit coarse NH_4 volume was estimated by multiplying the coarse volume (from LAS) by 0.1, the highest fraction of ammonium observed in coarse aerosol from prior studies (Kline et al., 2004; Cozic et al., 2008).

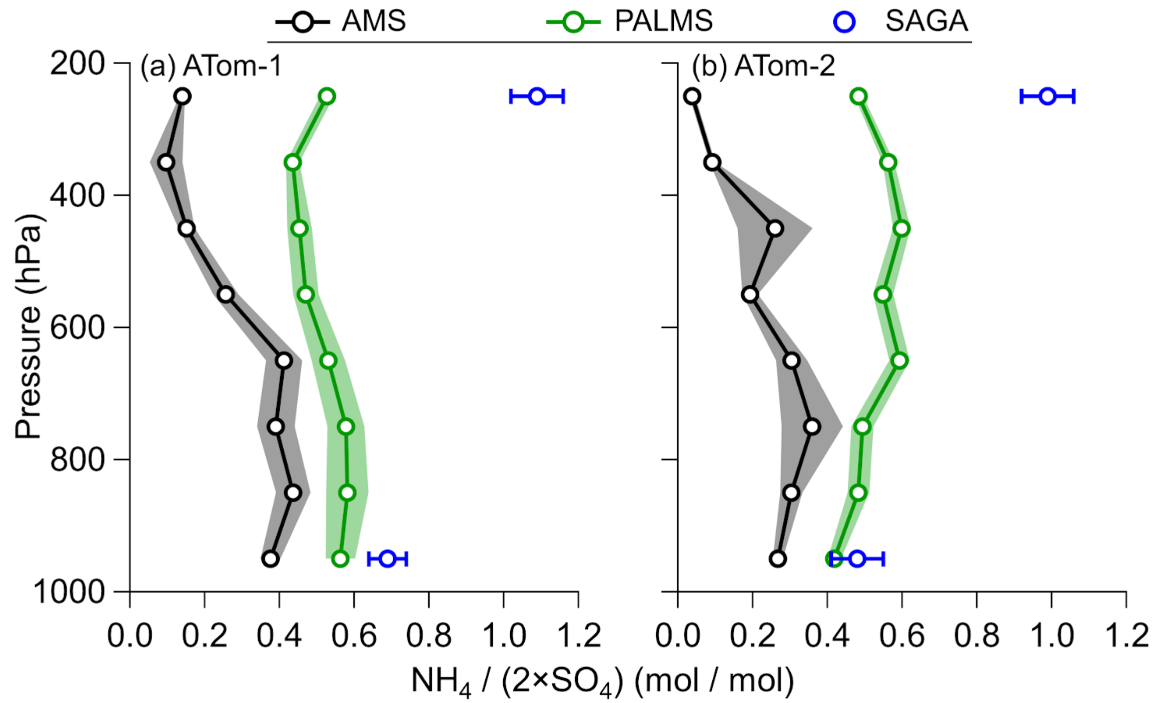

Figure S4. Similar to Fig. 3*, but for AMS, PALMS, and SAGA during ATom-1 (a) and ATom-2 (b). However, unlike* Fig. 3*, the x-axis is defined as $NH_4/(2\times SO_4)$ instead of $NH_4/(2\times SO_4 + NO_3)$, to be consistent with the data product from PALMS (Froyd et al., 2009). The shaded area and error bar is the standard error about the mean.*

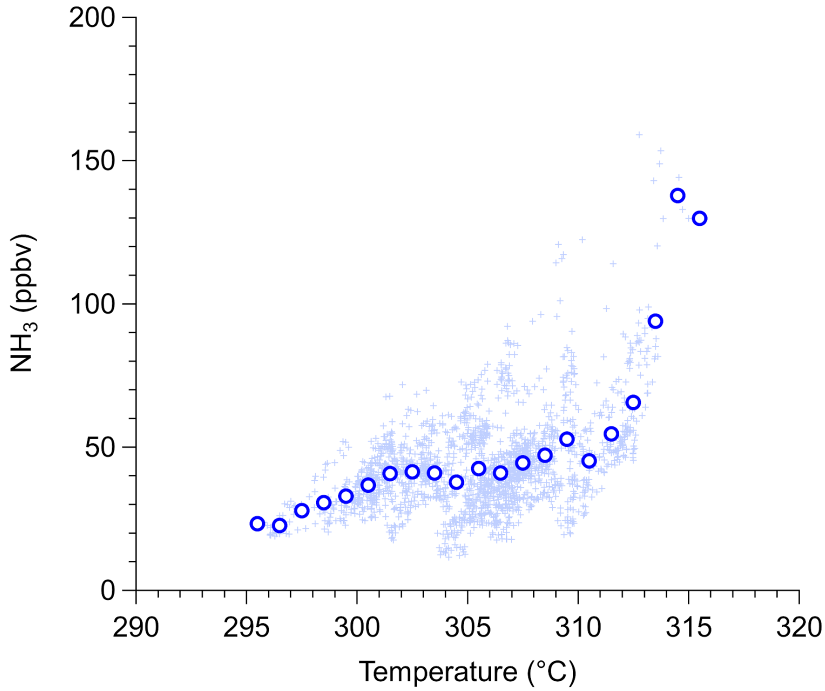

Figure S5. Gas-phase ammonia (NH_3) versus temperature, measured inside the cabin of the NASA DC-8, during FIREX-AQ. Light blue crosses are all data, and the blue circles are the binned data.

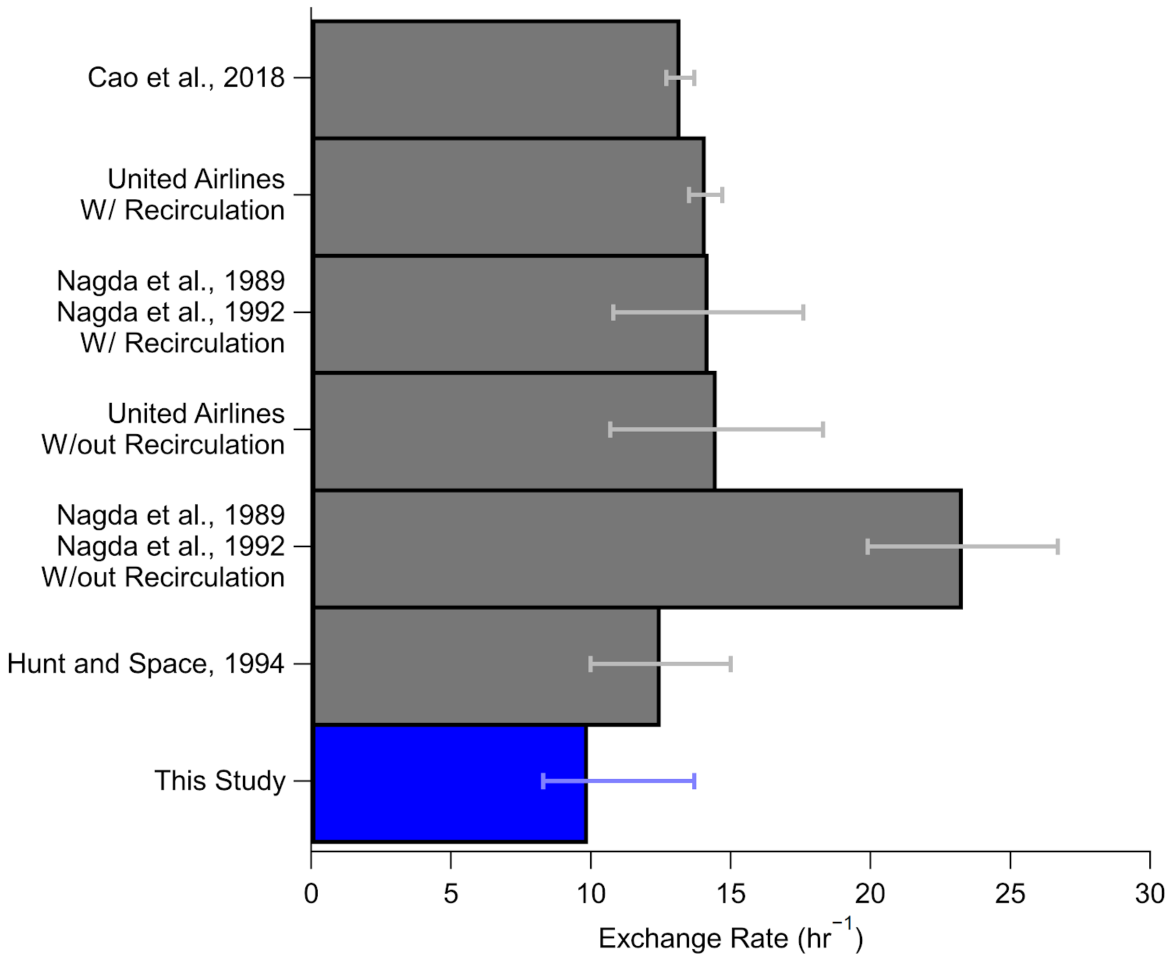

Figure S6. Exchange rates for air in the cabin of the DC-8 (blue), determined by the methods described in SI Sect. 5, compared with exchange rates cited in other studies from various aircraft cabins (Nagda et al., 1989, 1992; Hunt and Space, 1994; United Airlines, 1994; Cao et al., 2019).

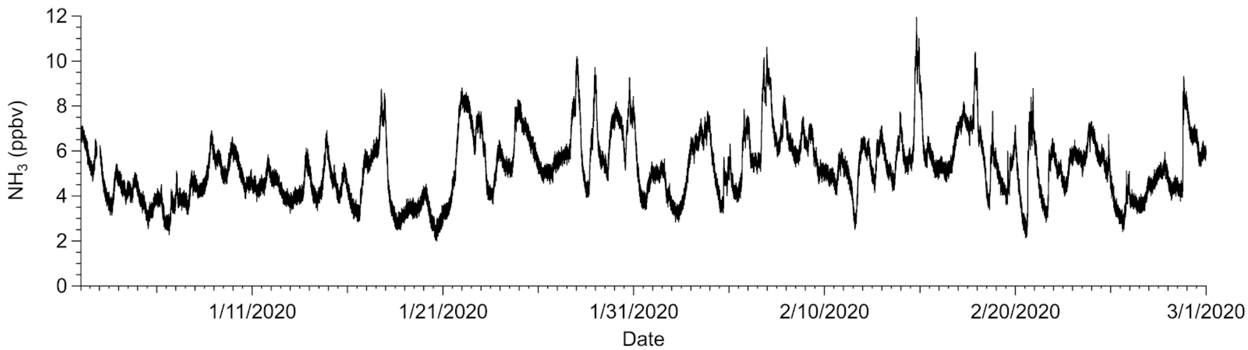

Figure S7. Gas-phase ammonia measured in the Jimenez Group laboratory at the University of Colorado at Boulder (room Cristol 343) for ~2 months.

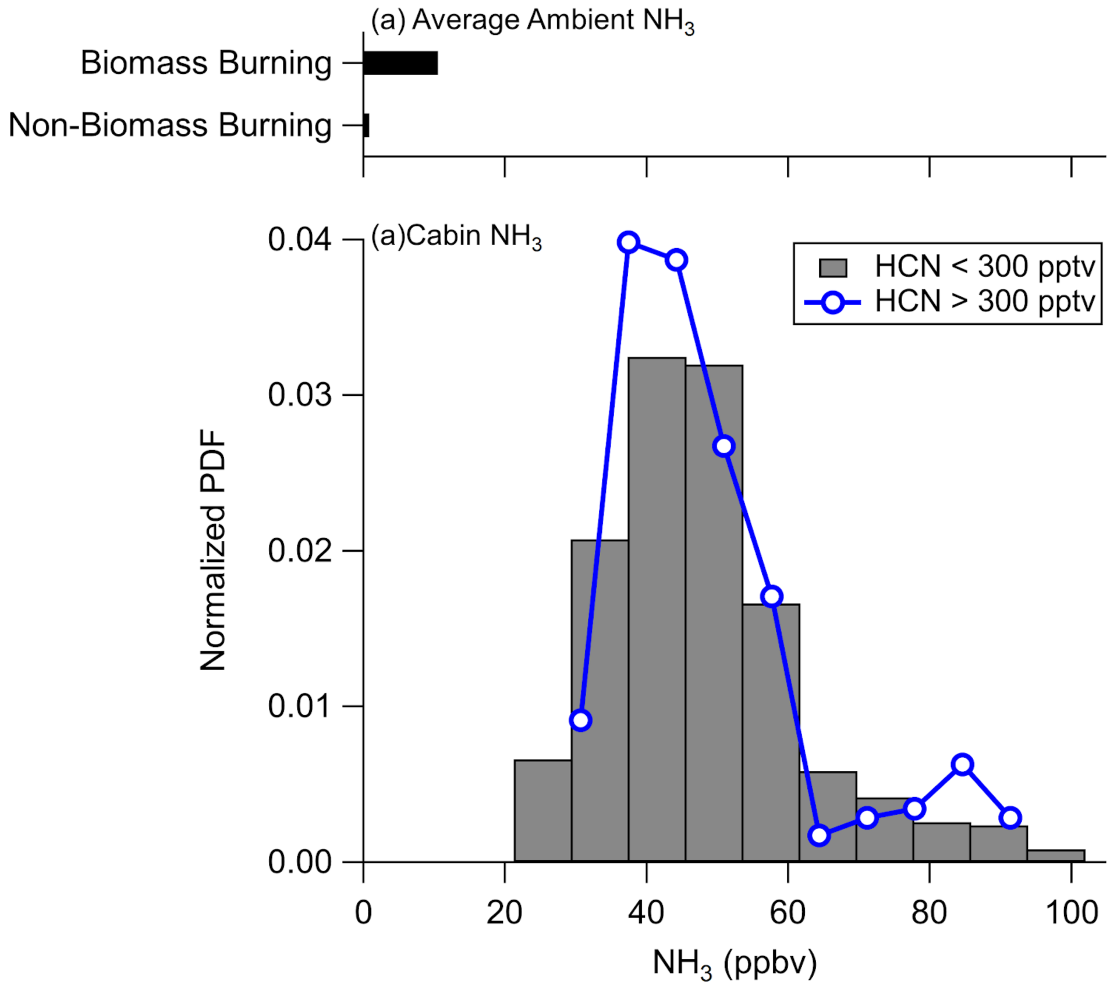

Figure S8. (top) Average ambient ammonia, measured by PTR-MS (Müller et al., 2014), sampled in air influenced (HCN > 300 pptv) and not influenced (HCN < 300 pptv) by biomass burning during the time period cabin was being sampled by Picarro. Note, this sampling was weighted towards the time period that the DC-8 was sampling agricultural fires, where the plumes were significantly smaller (seconds) versus the western fires at the beginning of the campaign (minutes - hours). (b) Normalized probability density function (PDF) of gas-phase ammonia (NH_3) measured in the cabin of the DC-8 during FIREX-AQ for when the DC-8 was sampling air influenced by biomass burning (HCN > 300 pptv) and not influenced by biomass burning (HCN < 300 pptv).

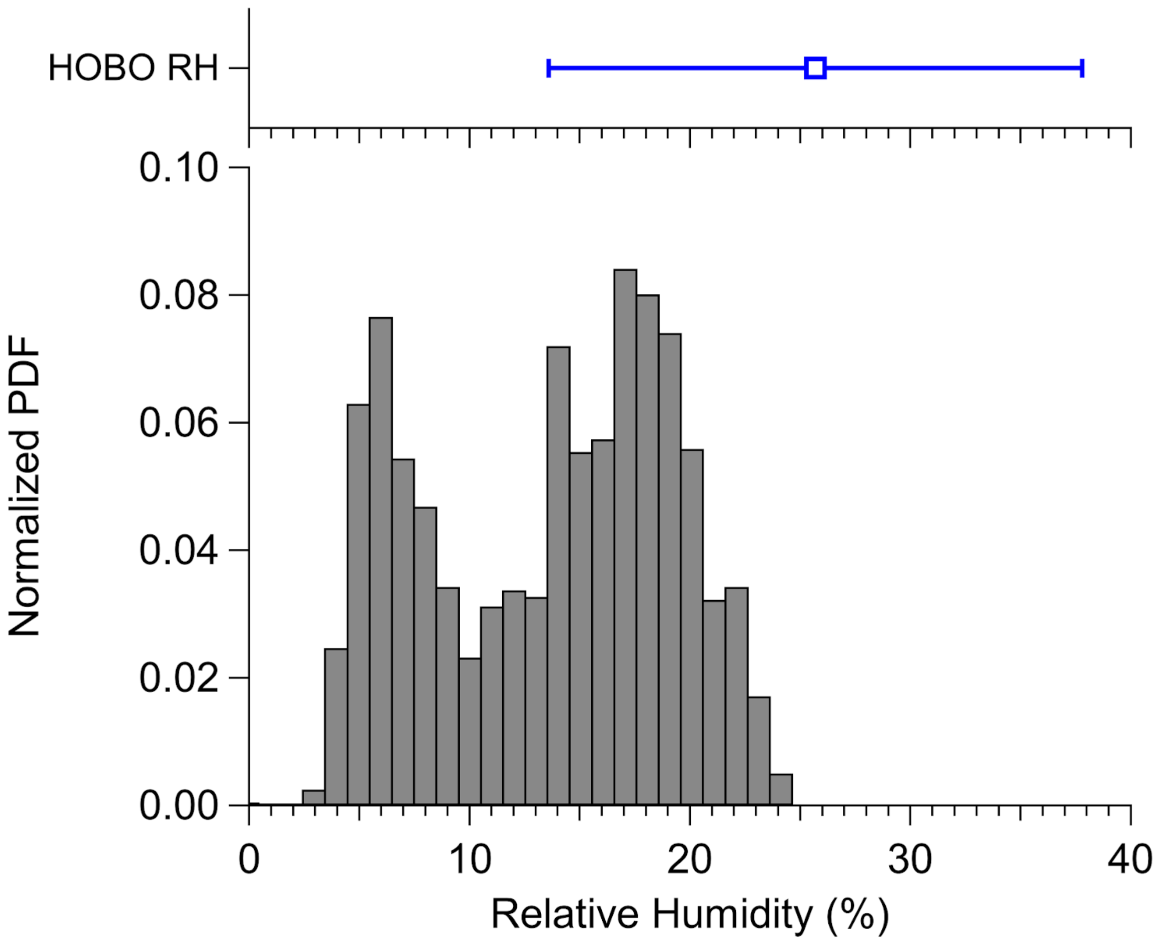

Figure S9. (top) Mean and standard deviation of relative humidity measured inside the NASA DC-8 cabin by the HOBO sensor. (bottom) Normalized probability distribution function (PDF) of relative humidity for inside the cabin of the NASA DC-8, calculated from the water vapor measured by the Picarro. Note that the periods of measurement of the two sensors do not completely overlap, therefore some difference is expected.

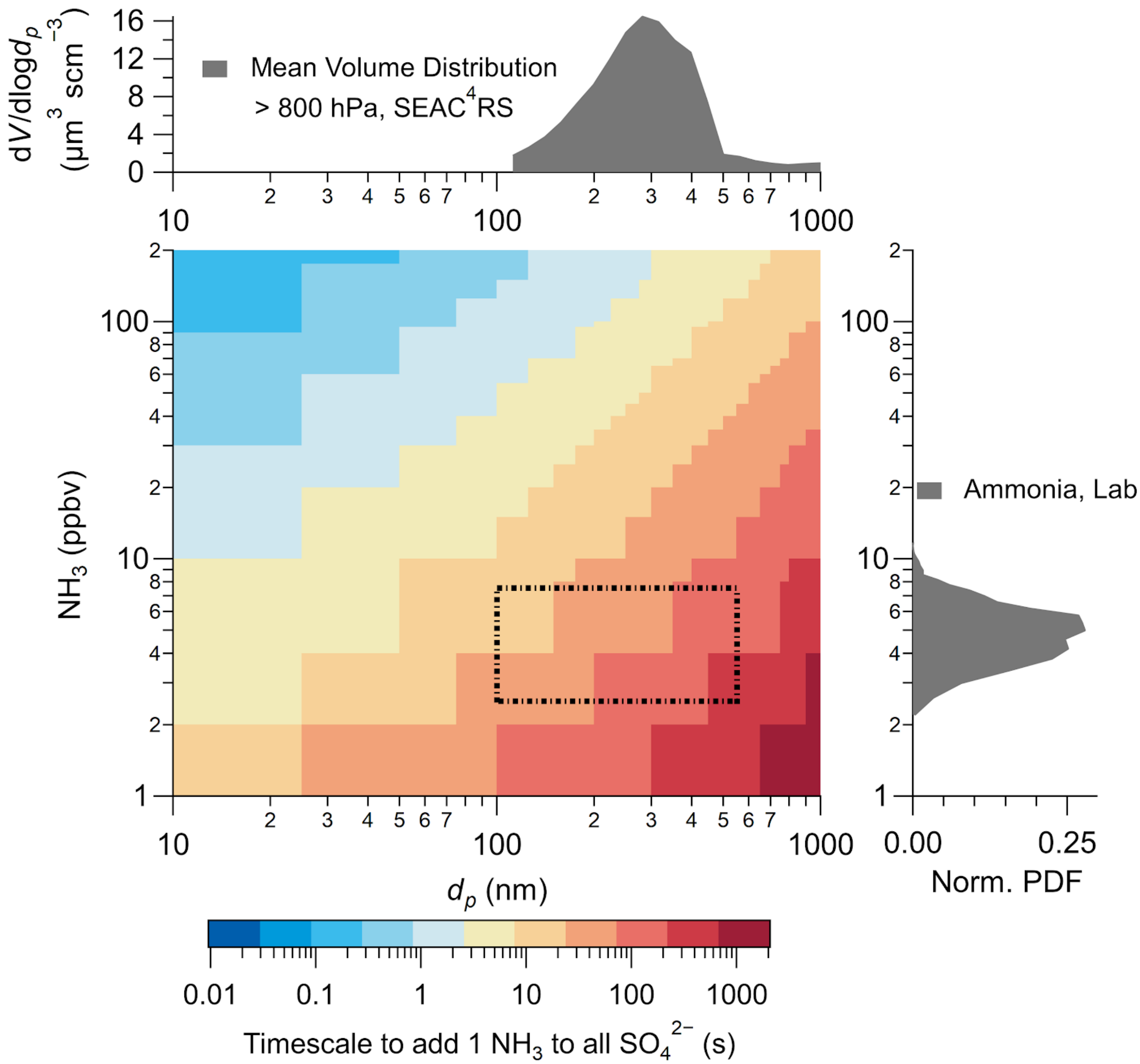

Figure S10. Same as Fig. 7*, but with histogram of laboratory ammonia (*Fig. S7*) and average boundary layer volume distribution, measured during SEAC^{4}RS.*

175

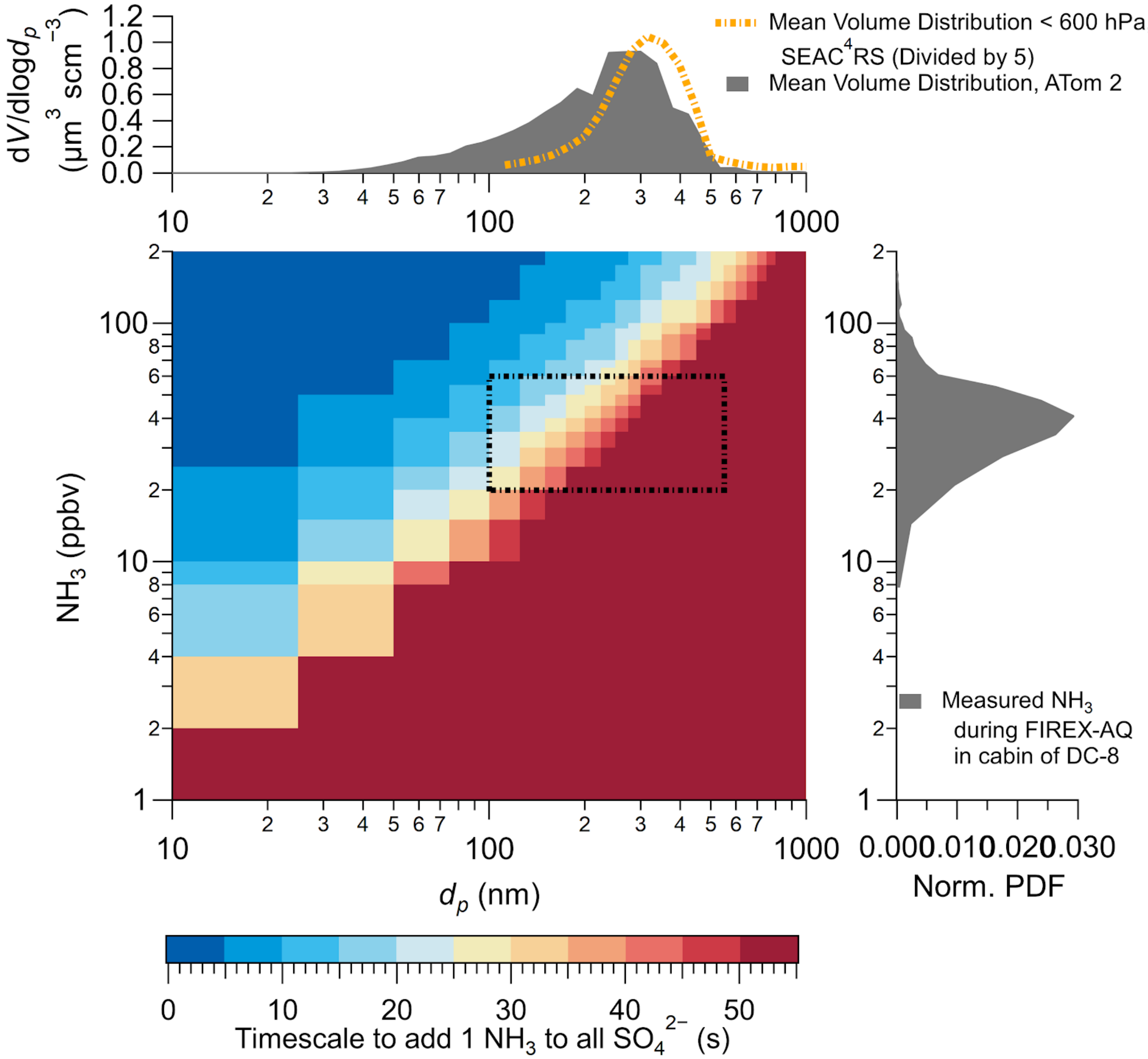

176 *Figure S11. Same as* Fig. 7*, but with accommodation coefficient of 0.1 instead of 1.*

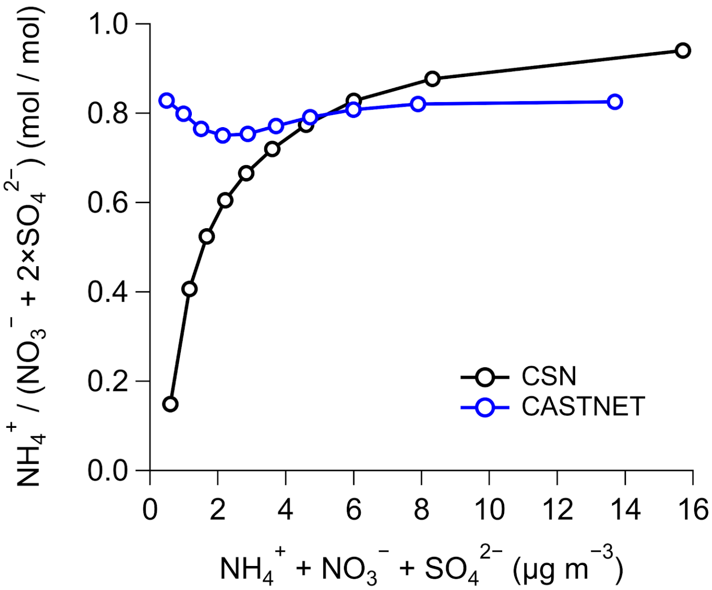

Figure S12. Comparison of binned data from Chemical Speciation Monitoring Network (CSN) (Solomon et al., 2000, 2014) and Clean air Status and Trends Network (CASTNET) (Lavery et al., 2009; Solomon et al., 2014) ammonium balance versus total inorganic mass concentration for the continental United States.

Tables

Table S1. *References for studies used in* Fig. 6.

Name of Study in Fig. 6	**Reference for Measurement/Predicted NH_3**
ATom-1 & -2	(Nault et al., 2020)
DISCOVER-AQ CO	(Battye et al., 2016)
CalNex	(Guo et al., 2017)
SOAS	(Guo et al., 2015)
WINTER	(Guo et al., 2016)
Cabauw Netherlands	(Guo et al., 2018)
Beijing	(Wang et al., 2016)
HomeChem	(Ampollini et al., 2019)
Average Homes	(Brauer et al., 1991; Atkins and Lee, 1993; Tidy and Neil Cape, 1993; Suh et al., 1994; Leaderer B P et al., 1999; Tuomainen et al., 2001; Fischer et al., 2003; Lunden et al., 2003; Järnström et al., 2006)
Average Offices	(Šišović et al., 1987; Salonen et al., 2009)
Average Schools	(Li and Harrison, 1990; Gomzi, 1999; Meininghaus et al., 2003)
ATHLETIC, All	(Finewax et al., 2020)

References

Ampollini, L., Katz, E. F., Bourne, S., Tian, Y., Novoselac, A., Goldstein, A. H., Lucic, G., Waring, M. S. and DeCarlo, P. F.: Observations and Contributions of Real-Time Indoor Ammonia Concentrations during HOMEChem, Environ. Sci. Technol., 53(15), 8591–8598, 2019.

Anon: DC-8 Airborne Science Experimenter Handbook, NASA. [online] Available from: https://espo.nasa.gov/sites/default/files/DC8_Experimenter_Handbook_Jan2011v2.pdf, 2011.

Atkins, D. H. F. and Lee, D. S.: Indoor concentrations of ammonia and the potential contribution of humans to atmospheric budgets, Atmos. Environ., 27(1), 1–7, 1993.

Battye, W. H., Bray, C. D., Aneja, V. P., Tong, D., Lee, P. and Tang, Y.: Evaluating ammonia (NH_3) predictions in the NOAA National Air Quality Forecast Capability (NAQFC) using in situ aircraft, ground-level, and satellite measurements from the DISCOVER-AQ Colorado campaign, Atmos. Environ., 140, 342–351, 2016.

Bey, I., Jacob, D. J., Yantosca, R. M., Logan, J. A., Field, B. D., Fiore, A. M., Li, Q., Liu, H. Y., Mickley, L. J. and Schultz, M. G.: Global modeling of tropospheric chemistry with assimilated meteorology: Model description and evaluation, J. Geophys. Res., 106(D19), 23073–23095, 2001.

Brauer, M., Koutrakis, P., Keeler, G. J. and Spengler, J. D.: Indoor and outdoor concentrations of inorganic acidic aerosols and gases, J. Air Waste Manage. Assoc., 41(2), 171–181, 1991.

Brundrett, G.: Comfort and health in commercial aircraft: a literature review, J. R. Soc. Promot. Health, 121(1), 29–37, 2001.

Cao, X., Zevitas, C. D., Spengler, J. D., Coull, B., McNeely, E., Jones, B., Loo, S. M., MacNaughton, P. and Allen, J. G.: The on-board carbon dioxide concentrations and ventilation performance in passenger cabins of US domestic flights, Indoor Built Environ., 28(6), 761–771, 2019.

Cozic, J., Verheggen, B., Weingartner, E., Crosier, J., Bower, K. N., Flynn, M., Coe, H., Henning, S., Steinbacher, M., Henne, S., Collaud Coen, M., Petzold, A. and Baltensperger, U.: Chemical composition of free tropospheric aerosol for PM_1 and coarse mode at the high alpine site Jungfraujoch, Atmos. Chem. Phys., 8(2), 407–423, 2008.

Crippa, M., Guizzardi, D., Muntean, M., Schaaf, E., Dentener, F., van Aardenne, J. A., Monni, S., Doering, U., Olivier, J. G. J., Pagliari, V. and Janssens-Maenhout, G.: Gridded emissions of air pollutants for the period 1970–2012 within EDGAR v4.3.2, Earth Syst. Sci. Data, 10(4), 1987–2013, 2018.

Finewax, Z., Pagonis, D., Claflin, M. S., Handschy, A. V., Brown, W. L., Ba, J. O. N., Lerner, B. M., Jimenez, J. L., Ziemann, P. J. and de Gouw, J. A.: Quantification and source characterization of volatile organic compounds from exercising and application of chlorine-based cleaning products in a university athletic center, Indoor Air, Submitted, 2020.

Fischer, M. L., Littlejohn, D., Lunden, M. M. and Brown, N. J.: Automated measurements of ammonia and nitric acid in indoor and outdoor air, Environ. Sci. Technol., 37(10), 2114–2119, 2003.

Fountoukis, C. and Nenes, A.: ISORROPIA II: a computationally efficient thermodynamic equilibrium model for K^+–Ca^{2+}–Mg^{2+}–NH_4^+–Na^+–SO_4^{2-}–NO_3^-–Cl^-–H_2O aerosols, Atmos. Chem. Phys., 7(17), 4639–4659, 2007.

Froyd, K. D., Murphy, D. M., Sanford, T. J., Thomson, D. S., Wilson, J. C., Pfister, L. and Lait, L.: Aerosol composition of the tropical upper troposphere, Atmos. Chem. Phys., 9(13), 4363–4385, 2009.

Giglio, L., Randerson, J. T. and van der Werf, G. R.: Analysis of daily, monthly, and annual burned area using the fourth-generation global fire emissions database (GFED4), J. Geophys. Res.: Biogeosci., 118(1), 317–328, 2013.

Gomzi, M.: Indoor air and respiratory health in preadolescent children, Atmos. Environ., 33(24), 4081–4086, 1999.

Guo, H., Xu, L., Bougiatioti, A., Cerully, K. M., Capps, S. L., Hite, J. R., Carlton, A. G., Lee, S.-H., Bergin, M. H., Ng, N. L., Nenes, A. and Weber, R. J.: Fine-particle water and pH in the southeastern United States, Atmos. Chem. Phys., 15(9), 5211–5228, 2015.

Guo, H., Sullivan, A. P., Campuzano-Jost, P., Schroder, J. C., Lopez-Hilfiker, F. D., Dibb, J. E., Jimenez, J. L., Thornton, J. A., Brown, S. S., Nenes, A. and Weber, R. J.: Fine particle pH and the partitioning of nitric acid during winter in the northeastern United States, J. Geophys. Res. D: Atmos., 121(17), 10,355–10,376, 2016.

Guo, H., Liu, J., Froyd, K. D., Roberts, J. M., Veres, P. R., Hayes, P. L., Jimenez, J. L., Nenes, A. and Weber, R. J.: Fine particle pH and gas–particle phase partitioning of inorganic species in Pasadena, California, during the 2010 CalNex campaign, Atmos. Chem. Phys., 17(9), 5703–5719, 2017.

Guo, H., Nenes, A. and Weber, R. J.: The underappreciated role of nonvolatile cations in aerosol ammonium-sulfate molar ratios, Atmos. Chem. Phys., 18(23), 17307–17323, 2018.

Healy, T. V., McKay, H. A. C., Pilbeam, A. and Scargill, D.: Ammonia and ammonium sulfate in the troposphere over the United Kingdom, J. Geophys. Res., 75(12), 2317–2321, 1970.

Hocking, M. B.: Indoor air quality: recommendations relevant to aircraft passenger cabins, Am. Ind. Hyg. Assoc. J., 59(7), 446–454, 1998.

Hunt, E. W. and Space, D. R.: The Airplane Cabin Environment: Issues Pertaining to Flight Attendant, in Comfort," International in-flight Service Management Organization Conference. [online] Available from:

http://citeseerx.ist.psu.edu/viewdoc/similar?doi=10.1.1.304.7321&type=cc (Accessed 25 March 2020), 1994.

Järnström, H., Saarela, K., Kalliokoski, P. and Pasanen, A.-L.: Reference values for indoor air pollutant concentrations in new, residential buildings in Finland, Atmos. Environ., 40(37), 7178–7191, 2006.

Kline, J., Huebert, B., Howell, S., Blomquist, B., Zhuang, J., Bertram, T. and Carrillo, J.: Aerosol composition and size versus altitude measured from the C-130 during ACE-Asia, J. Geophys. Res., 109(D19), 340, 2004.

Lavery, T. F., Rogers, C. M., Baumgardner, R. and Mishoe, K. P.: Intercomparison of Clean Air Status and Trends Network Nitrate and Nitric Acid Measurements with Data from Other Monitoring Programs, J. Air Waste Manag. Assoc., 59(2), 214–226, 2009.

Leaderer B P, Naeher L, Jankun T, Balenger K, Holford T R, Toth C, Sullivan J, Wolfson J M and Koutrakis P: Indoor, outdoor, and regional summer and winter concentrations of PM_{10}, $PM_{2.5}$, SO_4^{2-}, H^+, NH_4^+, NO_3^-, NH_3, and nitrous acid in homes with and without kerosene space heaters, Environ. Health Perspect., 107(3), 223–231, 1999.

Li, M., Weschler, C. J., Bekö, G., Wargocki, P., Lucic, G. and Williams, J.: Human Ammonia Emission Rates under Various Indoor Environmental Conditions, Environ. Sci. Technol., doi:10.1021/acs.est.0c00094, 2020.

Li, Y. and Harrison, R. M.: Comparison of indoor and outdoor concentrations of acid gases, ammonia and their associated salts, Environ. Technol., 11(4), 315–326, 1990.

Lunden, M. M., Revzan, K. L., Fischer, M. L., Thatcher, T. L., Littlejohn, D., Hering, S. V. and Brown, N. J.: The transformation of outdoor ammonium nitrate aerosols in the indoor environment, Atmos. Environ., 37(39), 5633–5644, 2003.

Meininghaus, R., Kouniali, A., Mandin, C. and Cicolella, A.: Risk assessment of sensory irritants in indoor air--a case study in a French school, Environ. Int., 28(7), 553–557, 2003.

Müller, M., Mikoviny, T., Feil, S., Haidacher, S., Hanel, G., Hartungen, E., Jordan, A., Märk, L., Mutschlechner, P., Schottkowsky, R., Sulzer, P., Crawford, J. H. and Wisthaler, A.: A compact PTR-ToF-MS instrument for airborne measurements of volatile organic compounds at high spatiotemporal resolution, , doi:10.5194/amt-7-3763-2014, 2014.

Nagda, N. L., Fortmann, R. C., Koontz, M. D., Baker, S. R. and Ginevan, M. E.: Airliner Cabin Environment: Contaminant Measurements, Health Risks, and Mitigation Options, US Department of Transportation., 1989.

Nagda, N. L., Koontz, M. D., Konheim, A. G. and Katharine Hammond, S.: Measurement of cabin air quality aboard commercial airliners, Atmospheric Environment. Part A. General Topics, 26(12), 2203–2210, 1992.

National Research Council: The Airliner Cabin Environment and the Health of Passengers and Crew, The National Academies Press, Washington, DC., 2002.

Nault, B. A., Campuzano-Jost, P., Jo, D., Day, D., Bahreini, R., Bian, H., Chin, M., Clegg, S., Colarco, P., Kodros, J., Lopez-Hilfiker, F., Marais, E., Middlebrook, A., Neuwman, A., Nowak, J., Pierce, J., Thornton, J., Tsigaridis, K., Jimenez, J. and ATom Science Team: Global Survey of Aerosol Acidity from Polluted to Remote Locations: Measurements and Comparisons with Global Models, , doi:10.5194/egusphere-egu2020-11366, 2020.

Pagonis, D., Price, D. J., Algrim, L. B., Day, D. A., Handschy, A. V., Stark, H., Miller, S. L., de Gouw, J., Jimenez, J. L. and Ziemann, P. J.: Time-Resolved Measurements of Indoor Chemical Emissions, Deposition, and Reactions in a University Art Museum, Environ. Sci. Technol., 53(9), 4794–4802, 2019.

Pye, H. O. T., Liao, H., Wu, S., Mickley, L. J., Jacob, D. J., Henze, D. K. and Seinfeld, J. H.: Effect of changes in climate and emissions on future sulfate-nitrate-ammonium aerosol levels in the United States, J. Geophys. Res., 114(D1), 1097, 2009.

Rumble, J. R., Ed.: CRC Handbook of Chemistry and Physics, 100th Edition, 2019 - 2020, Taylor & Francis Group., 2019.

Salonen, H. J., Pasanen, A.-L., Lappalainen, S. K., Riuttala, H. M., Tuomi, T. M., Pasanen, P. O., Bäck, B. C. and Reijula, K. E.: Airborne concentrations of volatile organic compounds, formaldehyde and ammonia in Finnish office buildings with suspected indoor air problems, J. Occup. Environ. Hyg., 6(3), 200–209, 2009.

Seinfeld., J. H. and Pandis, S. N.: Atmospheric Chemistry and Physics: From Air Pollution to Climate Change, Second., John Wiley & Sons, Inc., Hoboken, NJ USA., 2006.

Šišović, A., Šega, K. and Kalinić, N.: Indoor/outdoor relationship of ammonia concentrations in selected office buildings, Sci. Total Environ., 61, 73–77, 1987.

Solomon, P. A., Mitchell, W., Tolocka, M., Norris, G., Gemmill, D., Wiener, R., Vanderpool, R., Murdoch, R., Natarajan, S. and Hardison, E.: Evaluation of PM2.5 Chemical Speciation Samplers for Use in the EPA National PM2.5 Chemical Speciation Network, EPA., 2000.

Solomon, P. A., Crumpler, D., Flanagan, J. B., Jayanty, R. K. M., Rickman, E. E. and McDade, C. E.: U.S. national PM2.5 Chemical Speciation Monitoring Networks-CSN and IMPROVE: description of networks, J. Air Waste Manag. Assoc., 64(12), 1410–1438, 2014.

Suh, H. H., Koutrakis, P. and Spengler, J. D.: The relationship between airborne acidity and ammonia in indoor environments, J. Expo. Anal. Environ. Epidemiol., 4(1), 1–22, 1994.

Sutton, M. A., Dragosits, U., Tang, Y. S. and Fowler, D.: Ammonia emissions from non-agricultural sources in the UK, Atmos. Environ., 34(6), 855–869, 2000.

Tang, X., Misztal, P. K., Nazaroff, W. W. and Goldstein, A. H.: Volatile Organic Compound

Emissions from Humans Indoors, Environ. Sci. Technol., 50(23), 12686–12694, 2016.

Tidy, G. and Neil Cape, J.: Ammonia concentrations in houses and public buildings, Atmospheric Environment. Part A. General Topics, 27(14), 2235–2237, 1993.

Tuomainen, M., Pasanen, A.-L., Tuomainen, A., Jyrki Liesivuori and Juvonen, P.: Usefulness of the Finnish classification of indoor climate, construction and finishing materials: comparison of indoor climate between two new blocks of flats in Finland, Atmos. Environ., 35(2), 305–313, 2001.

United Airlines: Cabin Air Quality., 1994.

Vay, S. A., Woo, J.-H., Anderson, B. E., Thornhill, K. L., Blake, D. R., Westberg, D. J., Kiley, C. M., Avery, M. A., Sachse, G. W., Streets, D. G., Tsutsumi, Y. and Nolf, S. R.: Influence of regional-scale anthropogenic emissions on CO_2 distributions over the western North Pacific, J. Geophys. Res., 108(D20), 213, 2003.

Vay, S. A., Choi, Y., Vadrevu, K. P., Blake, D. R., Tyler, S. C., Wisthaler, A., Hecobian, A., Kondo, Y., Diskin, G. S., Sachse, G. W., Woo, J.-H., Weinheimer, A. J., Burkhart, J. F., Stohl, A. and Wennberg, P. O.: Patterns of CO_2 and radiocarbon across high northern latitudes during International Polar Year 2008, J. Geophys. Res., 116(D14), 4039, 2011.

Wang, G., Zhang, R., Gomez, M. E., Yang, L., Levy Zamora, M., Hu, M., Lin, Y., Peng, J., Guo, S., Meng, J., Li, J., Cheng, C., Hu, T., Ren, Y., Wang, Y., Gao, J., Cao, J., An, Z., Zhou, W., Li, G., Wang, J., Tian, P., Marrero-Ortiz, W., Secrest, J., Du, Z., Zheng, J., Shang, D., Zeng, L., Shao, M., Wang, W., Huang, Y., Wang, Y., Zhu, Y., Li, Y., Hu, J., Pan, B., Cai, L., Cheng, Y., Ji, Y., Zhang, F., Rosenfeld, D., Liss, P. S., Duce, R. A., Kolb, C. E. and Molina, M. J.: Persistent sulfate formation from London Fog to Chinese haze, Proc. Natl. Acad. Sci. U. S. A., 113(48), 13630–13635, 2016.

Webster, A.: DC-8 Floor Plan, FIREX-AQ ESPO [online] Available from: https://espo.nasa.gov/sites/default/files/documents/DC800XXX%2C%20Preliminary%20-%20FIREX-AQ%20Loading%20Floorplan%2C%204-4-19.pdf (Accessed 27 April 2020), 2019.